

TUTORIAL REVIEW

[View Article Online](#)  
[View Journal](#) | [View Issue](#)



Cite this: *RSC Sustainability*, 2024, **2**, 91

## Sustainability-driven photocatalysis: oxygen-doped $\text{g-C}_3\text{N}_4$ for organic contaminant degradation

Soumya Ranjan Mishra, Vishal Gadore and Md. Ahmaruzzaman \*

Due to its distinct electrical structure and environmental compatibility, graphitic carbon nitride ( $\text{g-C}_3\text{N}_4$ ) has become a viable photocatalyst for various applications. Significant initiatives are currently being implemented to enhance the photocatalytic activity of  $\text{g-C}_3\text{N}_4$  by adding oxygen dopants to its structure. The unique characteristics of oxygen-doped  $\text{g-C}_3\text{N}_4$  ( $\text{O}@g\text{-C}_3\text{N}_4$ ), including enhanced charge carrier mobility and changed electronic structure, make it especially appealing for photocatalytic applications. The synthetic techniques used to create  $\text{O}@g\text{-C}_3\text{N}_4$  are thoroughly examined in this paper, along with the structural changes brought on by oxygen doping and the processes underpinning its increased photocatalytic activity. The methods for adding oxygen atoms to the  $\text{g-C}_3\text{N}_4$  lattice are covered in the synthesis section, including solid-state processes, chemical vapor deposition, hydrothermal synthesis, co-precipitation, and post-treatment procedures. Using these techniques, the type and density of oxygen functional groups may be precisely controlled, allowing  $\text{O}@g\text{-C}_3\text{N}_4$ 's photocatalytic characteristics to be tailored.  $\text{O}@g\text{-C}_3\text{N}_4$ 's characteristics are discussed, emphasizing its modified electronic band structure, better surface reactivity, and enhanced light absorption abilities. Recent developments in the field are also presented, exhibiting cutting-edge techniques, including heteroatom doping, nanostructuring, and co-catalyst integration that further enhance  $\text{O}@g\text{-C}_3\text{N}_4$ 's photocatalytic capabilities. As a versatile photocatalyst,  $\text{O}@g\text{-C}_3\text{N}_4$  has been extensively reviewed in this study, emphasizing its synthesis processes, structural characteristics, and current developments in improving its photocatalytic activity. Our understanding of  $\text{O}@g\text{-C}_3\text{N}_4$  is deepened by this review's insights, which also open the door for future research into using the compound in environmentally friendly and sustainable technology.

Received 24th October 2023  
Accepted 1st December 2023

DOI: 10.1039/d3su00384a  
[rsc.li/rscsus](http://rsc.li/rscsus)



### Sustainability spotlight

The mounting challenges caused by the rapid development of urbanization and industry drive the urgent demand for wastewater treatment. As long as these trends continue, the volume of wastewater generated will rise, bringing with it additional toxins, heavy metals, and organic contaminants. The release of untreated or inadequately treated wastewater endangers ecosystems owing to pollution, eutrophication, and public health concerns. This paper demonstrates a dedication to sustainability in materials science and environmental remediation. The focus of the investigation on oxygen-doped  $\text{g-C}_3\text{N}_4$  ( $\text{O}@g\text{-C}_3\text{N}_4$ ) yields intriguing advances with evident implications for material sustainability and ecological preservation. The importance of  $\text{O}@g\text{-C}_3\text{N}_4$  in the development of sustainable solutions cannot be overstated. This material demonstrates its potential to reduce environmental pollution and dependency on energy-intensive, non-renewable resources by harnessing sunlight for photocatalytic breakdown of organic pollutants. Its catalytic characteristics provide an environmentally benign alternative to traditional pollution removal technologies, leading to a greener, more sustainable future. Furthermore, the synthesis strategies mentioned in this article underline the significance of resource efficiency. Researchers are leveraging on the ubiquity of carbon and nitrogen supplies by altering  $\text{g-C}_3\text{N}_4$  with oxygen, decreasing the requirement for rare or expensive elements. This strategy is consistent with sustainability goals, emphasizing resource stewardship while providing efficient pollution removal. The structural features of  $\text{O}@g\text{-C}_3\text{N}_4$  improve its sustainability credentials even further. The material's stability and durability provide long-term efficacy in environmental cleanup, decreasing the need for regular replacements and minimizing waste. Its chemical stability under varied climatic circumstances promotes the concept of sustainability by allowing it to perform over long periods of time. In summary, the study described in this paper on  $\text{O}@g\text{-C}_3\text{N}_4$  constitutes a significant step toward sustainability in materials science. This material provides an eco-friendly solution for the elimination of organic pollutants by utilizing renewable energy sources, optimizing resource utilization, and boosting long-term performance. Its ability to reduce environmental harm while also contributing to a more sustainable future emphasizes its critical role in tackling global ecological concerns.

## 1. Introduction

The urgent need for wastewater cleanup is motivated by the growing difficulties brought on by the fast expansion of

Department of Chemistry, National Institute of Technology, Silchar, 788010, Assam, India. E-mail: [mda2002@gmail.com](mailto:mda2002@gmail.com)

urbanization and industrialization.<sup>1</sup> As long as these trends continue, there will be an increase in the amount of wastewater produced, full of new toxins, heavy metals, and organic pollutants.<sup>2</sup> Ecosystems are seriously threatened by the discharge of untreated or insufficiently treated wastewater due to pollution, eutrophication, and public health issues. Adequate wastewater treatment is crucial to solving these urgent problems. Innovative technologies are being created to address the increasing complexity of wastewater compositions and to support sustainable water resource management.<sup>3</sup> These technologies include enhanced oxidation processes, membrane filtration, and biological treatments.<sup>4</sup> In addition to removing pollutants, these methods seek to conserve energy, recover priceless resources, and lessen the environmental effects of wastewater management. Researchers are making critical efforts to secure freshwater supplies, preserve ecosystems, and assure the welfare of populations worldwide by advancing wastewater cleanup.<sup>5</sup>

As a critical area of environmental research and technology, photodegradation is essential for reducing the harmful effects of organic pollutants and toxins on ecosystems and human health.<sup>6,7</sup> Advanced photocatalytic materials have drawn much attention because they provide effective and sustainable methods for removing resistant organic molecules from various environmental matrices.<sup>8,9</sup> As a competitor among these materials, oxygen-doped graphitic carbon nitride ( $\text{O}@g\text{-C}_3\text{N}_4$ ) has shown great promise in photodegradation.<sup>10</sup> With a thorough examination of its synthesis, characteristics, current developments, and applications in the photodegradation of organic pollutants, this review paper digs into the complex world of  $\text{O}@g\text{-C}_3\text{N}_4$ . It gives a thorough overview of the crucial role  $\text{O}@g\text{-C}_3\text{N}_4$  plays in tackling today's environmental concerns by illuminating the structural complexities and functional improvements made possible by oxygen doping. Additionally, this review thoroughly analyzes the most recent developments in the industry, providing insightful information on the material's advancing capabilities and its transformative potential to create a cleaner, more sustainable future.

## 2. Synthesis techniques for fabrication of $\text{O}@g\text{-C}_3\text{N}_4$

The promising material  $\text{O}@g\text{-C}_3\text{N}_4$  has prospective uses in various industries, including photocatalysis and energy storage.<sup>11</sup> Oxygen doping can improve an object's electrical characteristics and performance in multiple tasks. The following are some typical techniques for producing  $\text{O}@g\text{-C}_3\text{N}_4$ :

### 2.1. Solid state reaction

This process includes combining an oxygen source, such as oxalic acid dihydrate, with a precursor containing carbon and nitrogen, often melamine, and heating the mixture to high temperatures in a controlled environment.<sup>12</sup> During the heating step, *i.e.*, up to 550 °C for 4 hours at a ramp rate of 20 °C min<sup>-1</sup>, the oxygen source's oxygen is integrated into the  $\text{g-C}_3\text{N}_4$  lattice to form  $\text{O}@g\text{-C}_3\text{N}_4$ . The fabricated  $\text{O}@g\text{-C}_3\text{N}_4$  by Mishra *et al.*<sup>12</sup>

was used to photodegrade methylene blue, rhodamine B, and methyl orange under visible light irradiation. Moreover, using ascorbic acid as the source, Zhang *et al.*<sup>13</sup> manufactured  $\text{O}@g\text{-C}_3\text{N}_4$  and used the photocatalyst to remove chromium. As can be seen in Fig. 1a,<sup>13</sup> the concentration of oxygen rises in  $\text{O}@g\text{-C}_3\text{N}_4$ , and new C–O and N–C–O bond was observed compared to pristine  $\text{g-C}_3\text{N}_4$  (Fig. 1b–d).<sup>13</sup>

### 2.2. Chemical vapor deposition (CVD)

In CVD, as carried out by Chubenko *et al.*,<sup>14</sup> a suitable substrate and carbon, nitrogen, and oxygen precursor gas are injected into a reaction chamber. The gas-phase precursors break down and deposit  $\text{O}@g\text{-C}_3\text{N}_4$  onto the substrate at a regulated temperature and pressure. The oxygen doping resulted in the compression of the  $\text{g-C}_3\text{N}_4$  lattice, which could be ascribed to the slightly nonstoichiometric composition of the material.

### 2.3. Hydrothermal synthesis

In this process, a precursor solution, including the carbon, nitrogen, and oxygen sources, is enclosed in a high-pressure autoclave and cooked to a high temperature. The oxygen source in this approach is often hydrogen peroxide or urea peroxide. This technique facilitates the development of  $\text{O}@g\text{-C}_3\text{N}_4$  nanoparticles. According to Chen *et al.*,<sup>15</sup> the obtained  $\text{g-C}_3\text{N}_4$  powder (1 g) was combined with 100 mL of a 30 vol%  $\text{H}_2\text{O}_2$  solution using ultrasonic dispersion for 20 min. The mixture was then put into a Teflon-sealed autoclave and kept at 120 °C for 6 h. The finished product underwent centrifugation, washing, and 60 °C drying overnight. Fig. 1e (ref. 15) shows that the (002) diffraction peak of  $\text{O}@g\text{-C}_3\text{N}_4$  moved from 27.3° to 27.6° and was significantly sharper, demonstrating the relationship among the adjacent layers was bolstered, and the interplanar layered distance was reduced due to oxygen atoms doping. As further evidence that the  $\text{O}_2$  atoms are successfully incorporated into the  $\text{g-C}_3\text{N}_4$  framework, a fresh faint peak at 1208 cm<sup>-1</sup> originating from the tensile vibration of C–O is seen in the  $\text{O}@g\text{-C}_3\text{N}_4$  sample (Fig. 1f).<sup>15</sup>

### 2.4. Co-precipitation method

This process entails the co-precipitation of metal ions with a source of carbon, nitrogen, and oxygen. After that, the precipitate is thermally processed to create oxygen-doped  $\text{g-C}_3\text{N}_4$ .<sup>16</sup> Solgi *et al.*<sup>16</sup> fabricated  $\text{O}@g\text{-C}_3\text{N}_4$  using the same process and used oxalic acid as the oxygen source.

### 2.5. Ion exchange method

This process involves soaking pre-synthesized  $\text{g-C}_3\text{N}_4$  in an oxygen-ion-containing solution, such as one containing nitrate or sulfate ions. The oxygen ions swap out some nitrogen particles in the  $\text{g-C}_3\text{N}_4$  lattice through ion exchange, leading to oxygen doping. Researchers carried out similar work, as illustrated in Fig. 1g.<sup>17</sup>  $\text{HNO}_3$  was used as the oxygen-ion-containing solution, and  $\text{g-C}_3\text{N}_4$  was submerged and hydrothermally treated at 80 °C to form oxygen-doped  $\text{g-C}_3\text{N}_4$ .



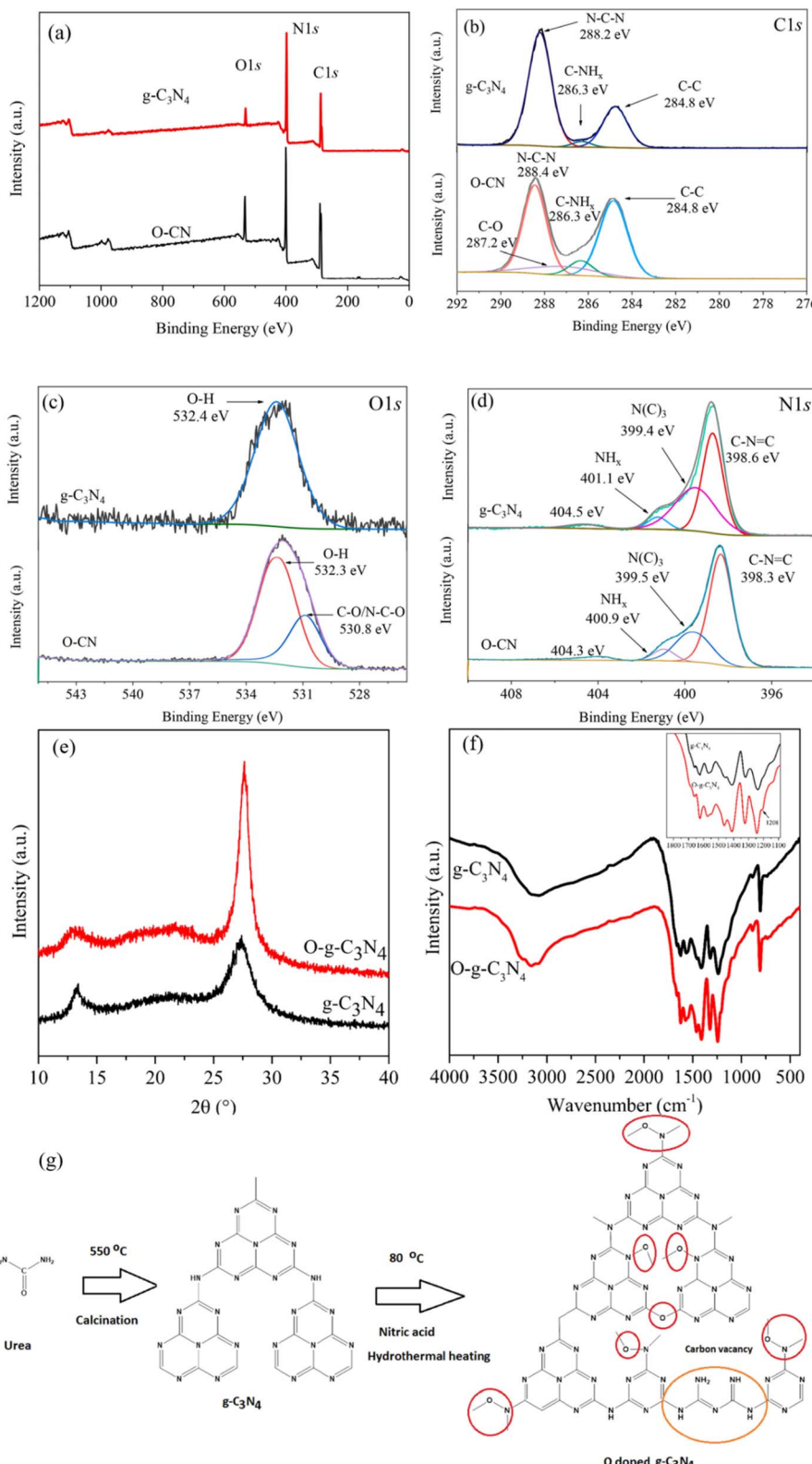


Fig. 1 (a) XPS survey spectra and short scan spectra of oxygen-doped  $\text{g-C}_3\text{N}_4$  with elements (b) C 1s, (c) O 1s, and (d) N 1s<sup>13</sup>; (e) XRD and (f) FTIR spectra of fabricated oxygen-doped  $\text{g-C}_3\text{N}_4$  (ref. 15); (g) ion exchange fabrication of oxygen-doped  $\text{g-C}_3\text{N}_4$ .<sup>17</sup>

The application's particular needs, the equipment and knowledge available, and the choice of synthesis process are all factors that can enhance the properties of a nanomaterial. Each technique has benefits and drawbacks, and depending on the synthesis path chosen, the characteristics of the O@g-C<sub>3</sub>N<sub>4</sub> material can change. Thus, the ideal approach for the study or industrial demands should be carefully selected.

### 3. Structure and properties of O@g-C<sub>3</sub>N<sub>4</sub>

#### 3.1. Structure of g-C<sub>3</sub>N<sub>4</sub> and O@g-C<sub>3</sub>N<sub>4</sub>

A modified form of graphitic carbon nitride (g-C<sub>3</sub>N<sub>4</sub>), oxygen-doped graphitic carbon nitride (O@g-C<sub>3</sub>N<sub>4</sub>), is distinguished by adding oxygen atoms to the g-C<sub>3</sub>N<sub>4</sub> lattice. It is crucial first to be familiar with the fundamental structure of pure g-C<sub>3</sub>N<sub>4</sub> to comprehend the structure of O@g-C<sub>3</sub>N<sub>4</sub>. The essential structure of g-C<sub>3</sub>N<sub>4</sub> characterizes it as a two-dimensional, layered substance made only of carbon (C) and nitrogen (N) atoms.<sup>18</sup> This structure is frequently compared to a polymer created when heptazine (C<sub>6</sub>N<sub>7</sub>) units are linked together by nitrogen atoms, resulting in a planar, honeycomb-like lattice resembling graphene.<sup>19</sup> The extraordinary lack of oxygen atoms in the structure of g-C<sub>3</sub>N<sub>4</sub>'s pure state highlights the substance's inherent purity. The short version of its chemical formula is (C<sub>3</sub>N<sub>4</sub>)<sub>n</sub>, where "n" stands for the number of repeating units that make up this polymeric structure, as can be illustrated in Fig. 2a.<sup>20</sup> Notably, the nitrogen atoms in g-C<sub>3</sub>N<sub>4</sub> adopt a sp<sup>2</sup>-hybridized configuration, which contributes to the lattice's planarity and gives it characteristic graphitic features.<sup>21</sup> As a result, g-C<sub>3</sub>N<sub>4</sub> is a material of significant attention in various scientific and technical applications.<sup>22</sup>

The intentional inclusion of oxygen atoms into the g-C<sub>3</sub>N<sub>4</sub> framework results in the structural configuration of O@g-C<sub>3</sub>N<sub>4</sub>. These inserted oxygen atoms take the form of oxygen-containing functional groups, such as hydroxyl (-OH), carbonyl (C=O), and carboxyl (-COOH) groups, among others. The two main methods for this oxygen doping are functional group attachment and substitutional incorporation. In the former, oxygen atoms take the place of a portion of the nitrogen atoms in the g-C<sub>3</sub>N<sub>4</sub> lattice, constituting a crucial part of the material's atomic structure, as described in Fig. 2b.<sup>23</sup> In the latter, oxygen atoms form oxygen-rich functional groups by adhering to the edges and flaws in the g-C<sub>3</sub>N<sub>4</sub> layers. Notably, the presence of these oxygen dopants significantly alters the electrical and molecular characteristics of O@g-C<sub>3</sub>N<sub>4</sub>. It promotes increased catalytic activity, allowing for greater reactivity in several chemical reactions.<sup>15</sup> Additionally, adding oxygen enhances the material's charge carrier mobility, a crucial component for its effectiveness in photocatalytic and electrical applications. Because of this, oxygen doping's structural changes play a vital role in enhancing O@g-C<sub>3</sub>N<sub>4</sub>'s functional capabilities and transforming it into a versatile substance of significant scientific and technological value.<sup>24</sup>

#### 3.2. Structural properties of O@g-C<sub>3</sub>N<sub>4</sub>

Several distinctive characteristics of the structural properties of O@g-C<sub>3</sub>N<sub>4</sub> substantially impact its functional capabilities.

Oxygen functional groups are one of O@g-C<sub>3</sub>N<sub>4</sub>'s most notable structural features. These functional groups, which include carboxyl (-COOH), carbonyl (C=O), and hydroxyl (-OH) groups, are thoughtfully incorporated into the material's structure as well as its surface.<sup>25</sup> These functional moieties are crucial in shaping O@g-C<sub>3</sub>N<sub>4</sub>'s chemical reactivity since they make interacting with other molecules easier and enable various chemical activities.

The electrical band structure of g-C<sub>3</sub>N<sub>4</sub> undergoes significant alterations due to oxygen doping. The optical and electrical characteristics of the material are critically affected by this change in the electronic environment.<sup>12</sup> It affects its ability to absorb light in various parts of the electromagnetic spectrum by causing absorption and emission spectra shifts. The improved photocatalytic and electronic performance of O@g-C<sub>3</sub>N<sub>4</sub> is primarily due to these modifications in the electronic structure, which make it easier for effective charge separation and migration to occur during photocatalytic processes and electronic device applications, as can be observed in Fig. 2c.<sup>15</sup>

Another essential structural property imparted by oxygen dopants is the development of active spots on the material's surface. Centres for catalytic and chemical processes are located at these active locations. Such sites make O@g-C<sub>3</sub>N<sub>4</sub> more reactive on its surface, increasing its potency for various chemical reactions.<sup>26</sup> Eliminating harmful organic pollutants from water and air sources is one application where this increased surface reactivity is very useful. O@g-C<sub>3</sub>N<sub>4</sub> has great promise for environmental remediation by offering many sites for pollutant adsorption and degradation.<sup>15</sup>

The adsorption of reagents and, as a result, oxygen doping can dramatically influence the photocatalytic reactivity of g-C<sub>3</sub>N<sub>4</sub>. Incorporating oxygen atoms into the g-C<sub>3</sub>N<sub>4</sub> lattice can result in the forming of oxygen-containing functional groups, which alters the surface characteristics and electronic structure.<sup>27</sup> Based on the nature of the oxygen dopants, this change can either increase or reduce reagent adsorption. For example, oxygen-containing groups may offer extra active sites for reagent adsorption, increasing total photocatalytic activity by allowing for improved interaction between the reagents and the photocatalyst.<sup>28</sup> Excessive oxygen doping, conversely, may produce non-reactive surface sites or modify the electronic structure so that reagent adsorption is hampered, resulting in a drop in photocatalytic reactivity. The effect of oxygen doping on reagent adsorption is critical in modifying g-C<sub>3</sub>N<sub>4</sub> surface chemistry for optimum photocatalytic performance in various applications.

In general, the structural characteristics of O@g-C<sub>3</sub>N<sub>4</sub> are closely related to its capabilities. The material's distinctive structural properties, which are the basis for its multifaceted utility in various scientific, technological, and environmental applications, are collectively defined by the existence of oxygen functional groups, changes in electronic structure, and the introduction of active surface sites.<sup>29</sup>



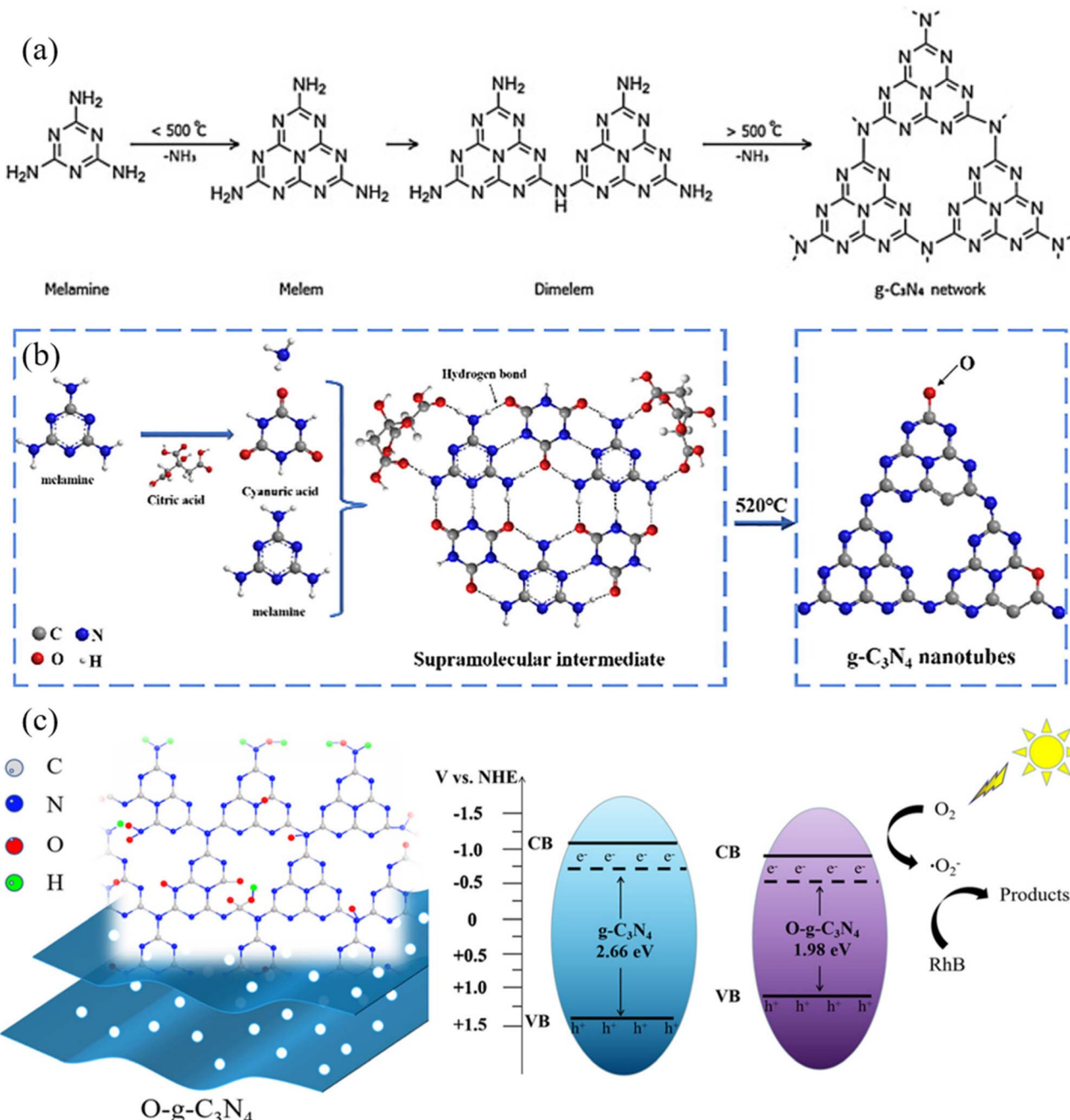


Fig. 2 Schematic illustration of structural changes during the synthesis of (a)  $\text{g-C}_3\text{N}_4$  (ref. 20) and (b)  $\text{O}@g\text{-C}_3\text{N}_4$  (ref. 23); (c) decrease in bandgap and increase in light absorption capacity due to oxygen doping onto  $\text{g-C}_3\text{N}_4$ .<sup>15</sup>

#### 4. Recent advancements in the photodegradation performance of $\text{O}@g\text{-C}_3\text{N}_4$

In the field of photodegradation,  $\text{O}@g\text{-C}_3\text{N}_4$  has recently become a compelling and adaptable photocatalyst.<sup>30</sup> These developments have considerably improved the material's ability to break down harmful organic contaminants and pollutants, revolutionizing the area. The sorts of oxygen functional groups

included in the lattice and the oxygen doping levels can now be precisely controlled thanks to advancements in synthesis techniques.  $\text{O}@g\text{-C}_3\text{N}_4$  now exhibits increased catalytic activity, expanded spectrum responsiveness, and better charge carrier separation, all of which have improved photocatalytic performance.<sup>31</sup> To further enhance  $\text{O}@g\text{-C}_3\text{N}_4$ 's photodegradation abilities, synergistic techniques have been investigated, including coupling it with co-catalysts or heteroatom doping. These recent developments highlight  $\text{O}@g\text{-C}_3\text{N}_4$  as a critical component in the search for environmentally friendly and

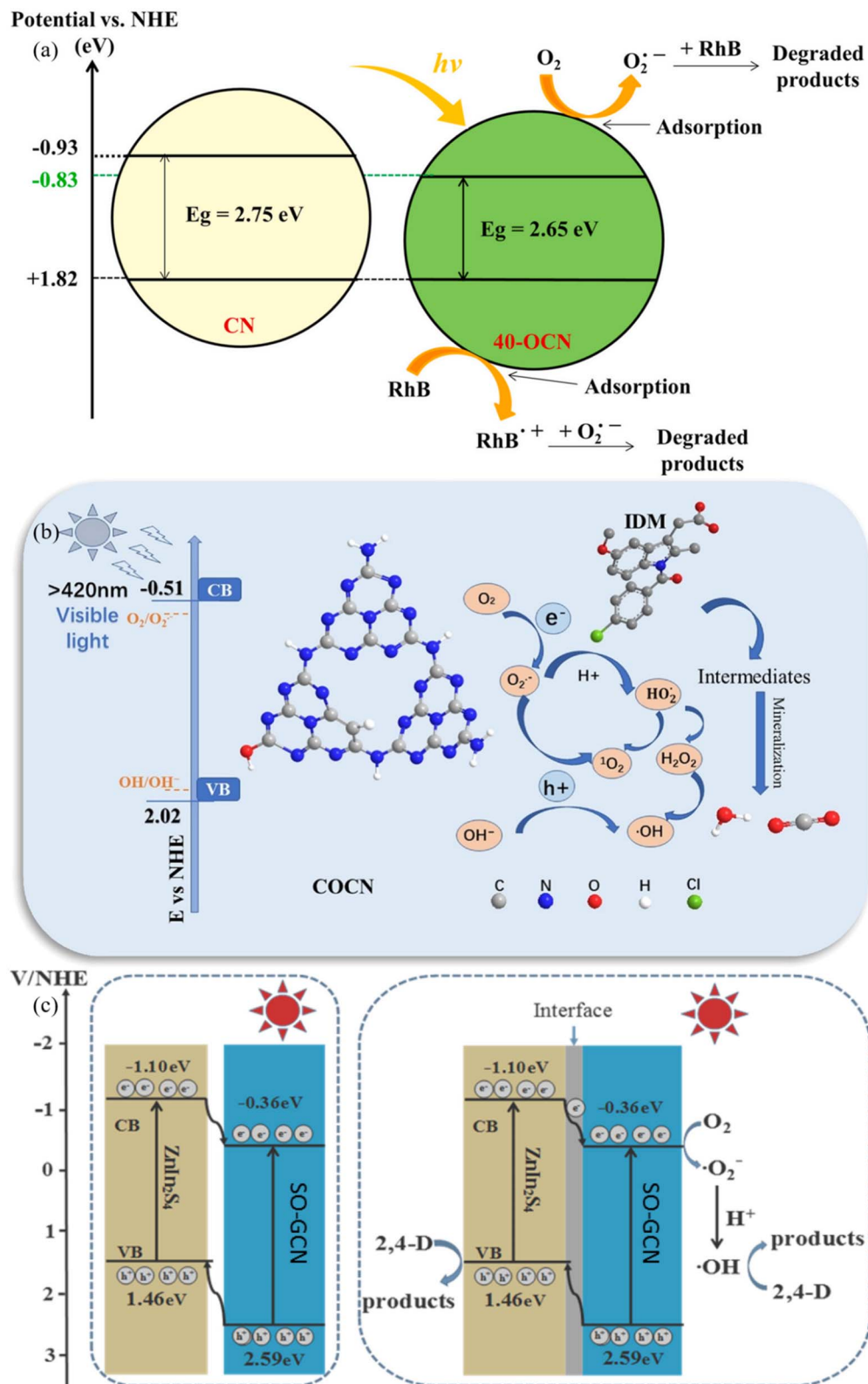


Fig. 3 (a) Degradation mechanism of pristine (a)  $\text{O}@g\text{-C}_3\text{N}_4$  (ref. 32), (b)  $\text{O}@g\text{-C}_3\text{N}_4$  developed on a 2D surface<sup>33</sup>, and (c)  $\text{O}@g\text{-C}_3\text{N}_4$ -based nanocomposite<sup>34</sup>

Table 1 Summary of the photocatalytic performance of O@g-C<sub>3</sub>N<sub>4</sub> and O@g-C<sub>3</sub>N<sub>4</sub>-based nanocomposite

| Photocatalyst  | Pollutants                      | Catalyst dosage (g L <sup>-1</sup> ) | Pollutant conc. (mg L <sup>-1</sup> )      | Time (min) | Efficiency (%) | Ref. |
|--|---------------------------------|--------------------------------------|--|------------|----------------|------|
| O@g-C <sub>3</sub> N <sub>4</sub>  | Methylene blue                  | 0.2                                  | 20   | 30         | 95.05 ± 2.17   | 12   |
| O@g-C <sub>3</sub> N <sub>4</sub>  | Rhodamine B                     | 0.2                                  | 20   | 30         | 97.79 ± 1.58   | 12   |
| O@g-C <sub>3</sub> N <sub>4</sub>  | Methyl orange                   | 0.2                                  | 20   | 30         | 89.77 ± 2.19   | 12   |
| O-g-C <sub>3</sub> N <sub>4</sub>  | Rhodamine B                     | 1                                    | 1.0 × 10 <sup>-5</sup> mol L <sup>-1</sup> | 70         | 90             | 15   |
| O@g-C <sub>3</sub> N <sub>4</sub>  | Tetracycline                    | 0.4                                  | 30   | 120        | 87.2           | 29   |
| O@g-C <sub>3</sub> N <sub>4</sub>  | Rhodamine B                     | 0.5                                  | 1.0 × 10 <sup>-5</sup> mol L <sup>-1</sup> | 15         | 98             | 35   |
| O@g-C <sub>3</sub> N <sub>4</sub>  | Rhodamine B                     | 1                                    | 30   | 140        | 94             | 32   |
| O@g-C <sub>3</sub> N <sub>4</sub>  | 2,4-Dinitrophenol               | 0.3                                  | 10   | 75         | 100            | 24   |
| O@g-C <sub>3</sub> N <sub>4</sub>  | Bisphenol A                     | 0.4                                  | 10   | 180        | 63             | 36   |
| O@g-C <sub>3</sub> N <sub>4</sub>  | Methylene blue                  | —                                    | —  | 180        | 81             | 25   |
| Carbon doped O@g-C <sub>3</sub> N <sub>4</sub>                                       | Indometacin                     | 0.4                                  | 4  | 60         | 98.9           | 33   |
| Carbon doped O@g-C <sub>3</sub> N <sub>4</sub>                                       | Bisphenol A                     | 1                                    | 10   | 240        | 97.85          | 37   |
| OCN/Py   | Tetracycline                    | 0.16                                 | 10   | 60         | 97.37          | 38   |
| Polyoxometalates/O@g-C <sub>3</sub> N <sub>4</sub>                                   | Sulfosalicylic acid             | 1                                    | 40   | 35         | 99             | 39   |
| Protonated g-C <sub>3</sub> N <sub>4</sub> /O-g-C <sub>3</sub> N <sub>4</sub>        | Deoxyxivalenol                  | —                                    | 10   | 150        | 86.6           | 40   |
| O@g-C <sub>3</sub> N <sub>4</sub> /NaBiS <sub>2</sub>                                | Methylene blue                  | 1                                    | 5  | 90         | 81             | 41   |
| O@g-C <sub>3</sub> N <sub>4</sub> /NaBiS <sub>2</sub>                                | Rhodamine B                     | 1                                    | 5  | 240        | 90             | 41   |
| In <sub>2</sub> O <sub>3</sub> /O@g-C <sub>3</sub> N <sub>4</sub>                    | Bisphenol A                     | 1                                    | —  | 180        | 91             | 42   |
| β-Bi <sub>2</sub> O <sub>3</sub> /O@g-C <sub>3</sub> N <sub>4</sub>                  | Bisphenol A                     | 0.5                                  | 15   | 180        | 98.7           | 43   |
| O@g-C <sub>3</sub> N <sub>4</sub> /CdS   | 2-Chlorophenol                  | —                                    | 10   | 60         | 100            | 44   |
| O-doped CN-M/CN-U  | Bisphenol A                     | —                                    | 5  | 90         | 75             | 45   |
| POCN/anatase TiO <sub>2</sub>  | Enrofloxacin                    | 1                                    | 10   | 60         | 98.5           | 26   |
| ZnIn <sub>2</sub> S <sub>4</sub> /SO-GCN   | 2,4-Dichloro phenoxyacetic acid | 0.4                                  | —  | 180        | 92             | 34   |
| O@g-C <sub>3</sub> N <sub>4</sub> /g-C <sub>3</sub> N <sub>4</sub> /TiO <sub>2</sub> | Gatifloxacin                    | 1                                    | 10   | 120        | 91.7           | 46   |

sustainable photodegradation solutions, holding great promise for addressing urgent environmental challenges like detoxifying industrial wastewater and removing persistent organic pollutants from water.

Pristine O-doped g-C<sub>3</sub>N<sub>4</sub> was fabricated by Tran *et al.*<sup>32</sup> for visible light photodegradation of rhodamine B. Compared to pure g-C<sub>3</sub>N<sub>4</sub>, the OCN compounds exhibit better photodegradation of rhodamine B. This is because the photocatalytic activity is improved due to a smaller bandgap energy and a slower recombination rate of generated electrons and holes, as illustrated in Fig. 3a.<sup>32</sup> Furthermore, O@g-C<sub>3</sub>N<sub>4</sub> was developed on carbon surface to photodegrade indometacin (IDM) under visible light irradiation by Zheng *et al.*<sup>33</sup> The improved photocatalytic activity may have been accredited to effective charge separation and a wider visible light absorption zone, as seen in Fig. 3b.<sup>33</sup> The carbon and oxygen-doped g-C<sub>3</sub>N<sub>4</sub> photocatalytic accomplishes excellent mineralization of IDM and offers a new approach to further strategize promising photocatalysts with exceptional wide spectral-responsive characteristics as a promising substitute for conventional water treatment technology. O@g-C<sub>3</sub>N<sub>4</sub>-based nanocomposites, as researched by Uddin *et al.*,<sup>34</sup> demonstrated a 3–5 times faster rate of 2,4-dichlorophenoxyacetic acid degradation under visible light irradiation (*i.e.*, 0.0112/min, by 30%-ZnIn<sub>2</sub>S<sub>4</sub>/SO-GCN), equated to pristine ZnIn<sub>2</sub>S<sub>4</sub> and SO-GCN. This is ascribed to the nanocomposite's harmonious effect in an exclusive 3D/2D heterojunction, which speeds up the e<sup>-</sup>/h<sup>+</sup> separation. The h<sup>+</sup> and ·OH species play a significant part in the breakdown of 2,4-dichlorophenoxyacetic acid over 30%-ZnIn<sub>2</sub>S<sub>4</sub>/SO-GCN, as illustrated in Fig. 3c.<sup>34</sup> Encouraging recent developments in O@g-C<sub>3</sub>N<sub>4</sub> for

photodegradation applications has, in summary, ushered in a new age of environmental remediation and sustainable pollution elimination. The material has evolved into a highly effective and promising photocatalyst, ready to solve the ever-growing ecological pollution and contamination difficulties. Table 1, provided below, summarises these cutting-edge advances in great detail.

## 5. Future perspective and conclusion

Future research and applications in oxygen-doped graphitic carbon nitride (O@g-C<sub>3</sub>N<sub>4</sub>) look promising. More research into precisely adjusting oxygen doping amounts and positions within the g-C<sub>3</sub>N<sub>4</sub> lattice will yield a more excellent knowledge of structure–property correlations. Enhancing photocatalytic effectiveness and expanding the material's uses require developing nanostructuring methods and exploring synergistic codoping with other heteroatoms. Further areas for investigation include O@g-C<sub>3</sub>N<sub>4</sub>'s ability to solve new environmental problems and its incorporation into scalable, affordable technologies for pollutant degradation, energy conversion, and environmental purification. Innovation, practical application, and critical role in long-term solutions for a cleaner and greener world are the hallmarks of O@g-C<sub>3</sub>N<sub>4</sub> research's future. Finally, O@g-C<sub>3</sub>N<sub>4</sub> has become a highly promising photocatalyst with enormous promise for resolving today's ecological and energy concerns. This article has emphasized the crucial significance of oxygen doping in cultivating the photocatalytic activity of O@g-C<sub>3</sub>N<sub>4</sub> by thoroughly studying synthesis techniques, structural alterations, and current developments. The g-C<sub>3</sub>N<sub>4</sub> lattice



is given special features by adding oxygen functions, including changed electronic band structures and better surface reactivity, dramatically increasing photocatalytic activity. These developments have a lot of potential for uses, including the oxidation of organic pollutants, the production of renewable energy, and environmental cleanup. Future advancements in O@ $\text{g-C}_3\text{N}_4$  research are expected to be interesting. It is anticipated that optimizing oxygen doping, investigating innovative co-doping procedures, and utilizing nanostructuring methods can further improve the material's performance. In addition, O@ $\text{g-C}_3\text{N}_4$  must be incorporated into practical tools and techniques to convert laboratory findings into workable solutions, ultimately paving the way for a cleaner and more sustainable future. O@ $\text{g-C}_3\text{N}_4$  is a tribute to the inventiveness of materials research and provides a look into the potential for functional materials to spur advancements in environmental rectification and energy conversion. Researchers and scientists are set to open new vistas in cutting-edge materials and sustainable technologies as the voyage of oxygen-doped  $\text{g-C}_3\text{N}_4$  continues.

## Conflicts of interest

There are no conflicts to declare.

## References

- 1 S. Roy, J. Darabdhara and M. Ahmaruzzaman, MoS<sub>2</sub> Nanosheets@Metal organic framework nanocomposite for enhanced visible light degradation and reduction of hazardous organic contaminants, *J. Cleaner Prod.*, 2023, **430**, 139517, DOI: [10.1016/J.JCLEPRO.2023.139517](https://doi.org/10.1016/J.JCLEPRO.2023.139517).
- 2 S. R. Mishra, V. Gadore and M. Ahmaruzzaman, A critical review on In<sub>2</sub>S<sub>3</sub>-based nanomaterial for emerging contaminants elimination through integrated adsorption-degradation technique: effect of reaction parameters and co-existing species, *J. Hazard. Mater. Lett.*, 2023, **4**, 100087, DOI: [10.1016/J.HAZL.2023.100087](https://doi.org/10.1016/J.HAZL.2023.100087).
- 3 V. Gadore, S. R. Mishra and M. Ahmaruzzaman, Metal sulphides and their heterojunctions for photocatalytic degradation of organic dyes-A comprehensive review, *Environ. Sci. Pollut. Res.*, 2023, 1–48, DOI: [10.1007/S11356-023-28753-W](https://doi.org/10.1007/S11356-023-28753-W).
- 4 S. R. Mishra and M. Ahmaruzzaman, Microplastics: Identification, Toxicity and Their Remediation from Aqueous Streams, *Sep. Purif. Rev.*, 2023, **52**(4), 283–304, DOI: [10.1080/15422119.2022.2096071](https://doi.org/10.1080/15422119.2022.2096071).
- 5 B. Bhattacharjee, B. Hazarika and M. Ahmaruzzaman, Visible-light-driven photocatalytic degradation of Rose Bengal and Methylene Blue using low-cost sawdust derived SnO<sub>2</sub> QDs@ $\text{g-C}_3\text{N}_4$ /biochar nanocomposite, *Environ. Sci. Pollut. Res.*, 2023, 1–20, DOI: [10.1007/S11356-023-30297-Y](https://doi.org/10.1007/S11356-023-30297-Y) METRICS.
- 6 A. K. Dey, S. R. Mishra and M. Ahmaruzzaman, Solar light-based advanced oxidation processes for degradation of methylene blue dye using novel Zn-modified CeO<sub>2</sub>@biochar, *Environ. Sci. Pollut. Res.*, 2023, **30**, 53887–53903, DOI: [10.1007/S11356-023-26183-2/TABLES/1](https://doi.org/10.1007/S11356-023-26183-2/TABLES/1).
- 7 S. R. Mishra, V. Gadore and M. Ahmaruzzaman, Inorganic-organic hybrid quantum dots for AOP-mediated photodegradation of ofloxacin and para-nitrophenol in diverse water matrices, *npj Clean Water*, 2023, **6**, 1–24, DOI: [10.1038/s41545-023-00291-5](https://doi.org/10.1038/s41545-023-00291-5).
- 8 S. R. Mishra, V. Gadore, R. Verma, K. R. B. Singh, J. Singh and M. Ahmaruzzaman, In<sub>2</sub>S<sub>3</sub> incorporated into CO<sub>3</sub>2-@Ni/Fe/Zn trimetallic LDH as a bi-functional novel nanomaterial for enzymatic urea sensing and removal of sulfur-containing pharmaceutical from aqueous streams, *Chem. Eng. J.*, 2023, **146207**, DOI: [10.1016/J.CEJ.2023.146207](https://doi.org/10.1016/J.CEJ.2023.146207).
- 9 K. Maeda, K. Teramura, D. Lu, T. Takata, N. Saito, Y. Inoue and K. Domen, Photocatalyst releasing hydrogen from water, *Nat.*, 2006, **440**(7082), 295, DOI: [10.1038/440295a](https://doi.org/10.1038/440295a).
- 10 S. Wang and J. Wang, Magnetic 2D/2D oxygen doped  $\text{g-C}_3\text{N}_4$ /biochar composite to activate peroxyomonosulfate for degradation of emerging organic pollutants, *J. Hazard. Mater.*, 2022, **423**, 127207, DOI: [10.1016/J.JHAZMAT.2021.127207](https://doi.org/10.1016/J.JHAZMAT.2021.127207).
- 11 T. J. Jiang, C. W. Luo, C. Xie, Y. H. Wei and A. Li, Synthesis of oxygen-doped graphitic carbon nitride and its application for the degradation of organic pollutants via dark Fenton-like reactions, *RSC Adv.*, 2020, **10**, 32906–32918, DOI: [10.1039/D0RA05202G](https://doi.org/10.1039/D0RA05202G).
- 12 S. R. Mishra, V. Gadore and M. Ahmaruzzaman, Influence of doped elements (O, K, and N) on melamine derived  $\text{g-C}_3\text{N}_4$ : insights into optical properties and photoactivity, *Int. J. Environ. Anal. Chem.*, 2023, DOI: [10.1080/03067319.2023.2260750](https://doi.org/10.1080/03067319.2023.2260750).
- 13 Z. Zhang, M. Zhang, F. Li, J. Tian and C. Yu, Fabrication, characterization of O doped  $\text{g-C}_3\text{N}_4$  materials via a green ascorbic acid-assisted calcination route, *Solid State Sci.*, 2021, **115**, 106605, DOI: [10.1016/J.SOLIDSTATESCIENCES.2021.106605](https://doi.org/10.1016/J.SOLIDSTATESCIENCES.2021.106605).
- 14 E. B. Chubenko, S. E. Maximov, C. D. Bui, V. T. Pham and V. E. Borisenko, Rapid chemical vapor deposition of graphitic carbon nitride films, *Materialia*, 2023, **28**, 101724, DOI: [10.1016/J.MTLA.2023.101724](https://doi.org/10.1016/J.MTLA.2023.101724).
- 15 M. Chen, R. Bai, P. Jin, J. Li, Y. Yan, A. Peng and J. He, A facile hydrothermal synthesis of few-layer oxygen-doped  $\text{g-C}_3\text{N}_4$  with enhanced visible light-responsive photocatalytic activity, *J. Alloys Compd.*, 2021, **869**, 159292, DOI: [10.1016/J.JALLOCOM.2021.159292](https://doi.org/10.1016/J.JALLOCOM.2021.159292).
- 16 S. Solgi, M. S. Seyed Dorraji, S. F. Hosseini, M. H. Rasoulifard, I. Hajimiri and A. Amani-Ghadim, Improvement of microwave absorption properties of polyester coatings using NiFe<sub>2</sub>O<sub>4</sub>, X-doped  $\text{g-C}_3\text{N}_4$  (X = S, P, and O), and MTiO<sub>3</sub> (M = Fe, Mg, and Zn) nanofillers, *Sci. Rep.*, 2021, **11**, 1–13, DOI: [10.1038/s41598-021-98666-6](https://doi.org/10.1038/s41598-021-98666-6).
- 17 C. Saka, Surface modification with oxygen doping of  $\text{g-C}_3\text{N}_4$  nanoparticles by carbon vacancy for efficient dehydrogenation of sodium borohydride in methanol, *Fuel*, 2022, **310**, 122444, DOI: [10.1016/J.FUEL.2021.122444](https://doi.org/10.1016/J.FUEL.2021.122444).
- 18 H. Luo, T. Shan, J. Zhou, L. Huang, L. Chen, R. Sa, Y. Yamauchi, J. You, Y. Asakura, Z. Yuan and H. Xiao, Controlled synthesis of hollow carbon ring incorporated  $\text{g-C}_3\text{N}_4$  tubes for boosting photocatalytic H<sub>2</sub>O<sub>2</sub> production,



*Appl. Catal., B*, 2023, **337**, 122933, DOI: [10.1016/J.APCATB.2023.122933](https://doi.org/10.1016/J.APCATB.2023.122933).

19 M. Ahmaruzzaman and S. R. Mishra, Photocatalytic performance of g-C3N4 based nanocomposites for effective degradation/removal of dyes from water and wastewater, *Mater. Res. Bull.*, 2021, **143**, 111417, DOI: [10.1016/J.MATERRESBULL.2021.111417](https://doi.org/10.1016/J.MATERRESBULL.2021.111417).

20 I. Papailias, T. Giannakopoulou, N. Todorova, D. Demotikali, T. Vaimakis and C. Trapalis, Effect of processing temperature on structure and photocatalytic properties of g-C3N4, *Appl. Surf. Sci.*, 2015, **358**, 278–286, DOI: [10.1016/J.APSUSC.2015.08.097](https://doi.org/10.1016/J.APSUSC.2015.08.097).

21 J. Jia, Q. Zhang, K. Li, Y. Zhang, E. Liu and X. Li, Recent advances on g-C3N4-based Z-scheme photocatalysts: structural design and photocatalytic applications, *Int. J. Hydrogen Energy*, 2023, **48**, 196–231, DOI: [10.1016/J.IJHYDENE.2022.09.272](https://doi.org/10.1016/J.IJHYDENE.2022.09.272).

22 D. Mohanta, A. Mahanta, S. R. Mishra, S. Jasimuddin and M. Ahmaruzzaman, Novel SnO<sub>2</sub>@ZIF-8/gC3N4 nanohybrids for excellent electrochemical performance towards sensing of p-nitrophenol, *Environ. Res.*, 2021, **197**, 111077, DOI: [10.1016/J.ENVRES.2021.111077](https://doi.org/10.1016/J.ENVRES.2021.111077).

23 Y. Zhang, Z. Chen, J. Li, Z. Lu and X. Wang, Self-assembled synthesis of oxygen-doped g-C3N4 nanotubes in enhancement of visible-light photocatalytic hydrogen, *J. Energy Chem.*, 2021, **54**, 36–44, DOI: [10.1016/J.JECHEM.2020.05.043](https://doi.org/10.1016/J.JECHEM.2020.05.043).

24 Y. Zeng, X. Liu, C. Liu, L. Wang, Y. Xia, S. Zhang, S. Luo and Y. Pei, Scalable one-step production of porous oxygen-doped g-C3N4 nanorods with effective electron separation for excellent visible-light photocatalytic activity, *Appl. Catal., B*, 2018, **224**, 1–9, DOI: [10.1016/J.APCATB.2017.10.042](https://doi.org/10.1016/J.APCATB.2017.10.042).

25 J. Li, B. Shen, Z. Hong, B. Lin, B. Gao and Y. Chen, A facile approach to synthesize novel oxygen-doped g-C3N4 with superior visible-light photoreactivity, *Chem. Commun.*, 2012, **48**, 12017–12019, DOI: [10.1039/C2CC35862J](https://doi.org/10.1039/C2CC35862J).

26 J. Huang, D. Li, R. Li, P. Chen, Q. Zhang, H. Liu, W. Lv, G. Liu and Y. Feng, One-step synthesis of phosphorus/oxygen co-doped g-C3N4/anatase TiO<sub>2</sub> Z-scheme photocatalyst for significantly enhanced visible-light photocatalysis degradation of enrofloxacin, *J. Hazard. Mater.*, 2020, **386**, 121634, DOI: [10.1016/J.JHAZMAT.2019.121634](https://doi.org/10.1016/J.JHAZMAT.2019.121634).

27 H. Tang, Z. Xia, R. Chen, Q. Liu and T. Zhou, Oxygen doped g-C3N4 with nitrogen vacancy for enhanced photocatalytic hydrogen evolution, *Chem.-Asian J.*, 2020, **15**, 3456–3461, DOI: [10.1002/ASIA.202000912](https://doi.org/10.1002/ASIA.202000912).

28 J. Zhang, B. Xin, C. Shan, W. Zhang, D. D. Dionysiou and B. Pan, Roles of oxygen-containing functional groups of O-doped g-C3N4 in catalytic ozonation: quantitative relationship and first-principles investigation, *Appl. Catal., B*, 2021, **292**, 120155, DOI: [10.1016/J.APCATB.2021.120155](https://doi.org/10.1016/J.APCATB.2021.120155).

29 Y. Shi, L. Li, H. Sun, Z. Xu, Y. Cai, W. Shi, F. Guo and X. Du, Engineering ultrathin oxygen-doped g-C3N4 nanosheet for boosted photoredox catalytic activity based on a facile thermal gas-shocking exfoliation effect, *Sep. Purif. Technol.*, 2022, **292**, 121038, DOI: [10.1016/J.SEPPUR.2022.121038](https://doi.org/10.1016/J.SEPPUR.2022.121038).

30 H. Xie, Y. Zheng, X. Guo, Y. Liu, Z. Zhang, J. Zhao, W. Zhang, Y. Wang and Y. Huang, Rapid Microwave Synthesis of Mesoporous Oxygen-Doped g-C3N4 with Carbon Vacancies for Efficient Photocatalytic H<sub>2</sub>O<sub>2</sub> Production, *ACS Sustain. Chem. Eng.*, 2021, **9**, 6788–6798, DOI: [10.1021/ACSSUSCHEMENG.1C01012/ASSET/IMAGES/LARGE/SC1C01012\\_0012.JPG](https://doi.org/10.1021/ACSSUSCHEMENG.1C01012/ASSET/IMAGES/LARGE/SC1C01012_0012.JPG).

31 F. Wang, J. Xu, Z. Wang, Y. Lou, C. Pan and Y. Zhu, Unprecedentedly efficient mineralization performance of photocatalysis-self-Fenton system towards organic pollutants over oxygen-doped porous g-C3N4 nanosheets, *Appl. Catal., B*, 2022, **312**, 121438, DOI: [10.1016/J.APCATB.2022.121438](https://doi.org/10.1016/J.APCATB.2022.121438).

32 D. A. Tran, C. T. Nguyen Pham, T. Nguyen Ngoc, H. Nguyen Phi, Q. T. Hoai Ta, D. H. Truong, V. T. Nguyen, H. H. Luc, L. T. Nguyen, N. N. Dao, S. J. Kim and V. Vo, One-step synthesis of oxygen doped g-C3N4 for enhanced visible-light photodegradation of Rhodamine B, *J. Phys. Chem. Solids*, 2021, **151**, 109900, DOI: [10.1016/J.JPCS.2020.109900](https://doi.org/10.1016/J.JPCS.2020.109900).

33 X. Zheng, Q. Zhang, T. Chen, Y. Wu, J. Hao, C. Tan, P. Chen, F. Wang, H. Liu, W. Lv and G. Liu, A novel synthetic carbon and oxygen doped stalactite-like g-C3N4 for broad-spectrum-driven indometacin degradation, *J. Hazard. Mater.*, 2020, **386**, 121961, DOI: [10.1016/J.JHAZMAT.2019.121961](https://doi.org/10.1016/J.JHAZMAT.2019.121961).

34 A. Uddin, T. Muhammed, Z. Guo, J. Gu, H. Chen and F. Jiang, Hydrothermal synthesis of 3D/2D heterojunctions of ZnIn<sub>2</sub>S<sub>4</sub>/oxygen doped g-C3N4 nanosheet for visible light driven photocatalysis of 2,4-dichlorophenoxyacetic acid degradation, *J. Alloys Compd.*, 2020, **845**, 156206, DOI: [10.1016/J.JALLCOM.2020.156206](https://doi.org/10.1016/J.JALLCOM.2020.156206).

35 F. Wei, Y. Liu, H. Zhao, X. Ren, J. Liu, T. Hasan, L. Chen, Y. Li and B. L. Su, Oxygen self-doped g-C<sub>3</sub>N<sub>4</sub> with tunable electronic band structure for unprecedentedly enhanced photocatalytic performance, *Nanoscale*, 2018, **10**, 4515–4522, DOI: [10.1039/C7NR09660G](https://doi.org/10.1039/C7NR09660G).

36 R. Tang, R. Ding and X. Xie, Preparation of oxygen-doped graphitic carbon nitride and its visible-light photocatalytic performance on bisphenol A degradation, *Water Sci. Technol.*, 2018, **78**, 1023–1033, DOI: [10.2166/WST.2018.361](https://doi.org/10.2166/WST.2018.361).

37 L. Jing, D. Wang, M. He, Y. Xu, M. Xie, Y. Song, H. Xu and H. Li, An efficient broad spectrum-driven carbon and oxygen co-doped g-C3N4 for the photodegradation of endocrine disrupting: mechanism, degradation pathway, DFT calculation and toluene selective oxidation, *J. Hazard. Mater.*, 2021, **401**, 123309, DOI: [10.1016/J.JHAZMAT.2020.123309](https://doi.org/10.1016/J.JHAZMAT.2020.123309).

38 H. Fang, J. Gao, J. Wang, J. Xu and L. Wang, Oxygen-doped and pyridine-grafted g-C3N4 for visible-light driven peroxyomonosulfate activation: insights of enhanced tetracycline degradation mechanism, *Sep. Purif. Technol.*, 2023, **314**, 123565, DOI: [10.1016/J.SEPPUR.2023.123565](https://doi.org/10.1016/J.SEPPUR.2023.123565).

39 X. An, S. Wu, Q. Tang, H. Lan, Y. Tang, H. Liu and J. Qu, Strongly coupled polyoxometalates/oxygen doped g-C3N4 nanocomposites as Fenton-like catalysts for efficient photodegradation of sulfosalicylic acid, *Catal. Commun.*, 2018, **112**, 63–67, DOI: [10.1016/J.CATCOM.2018.03.013](https://doi.org/10.1016/J.CATCOM.2018.03.013).



40 X. Chen, B. Chu, Q. Gu, H. Liu, C. Li, W. Li, J. Lu and D. Wu, Facile fabrication of protonated g-C<sub>3</sub>N<sub>4</sub>/oxygen-doped g-C<sub>3</sub>N<sub>4</sub> homojunction with enhanced visible photocatalytic degradation performance of deoxynivalenol, *J. Environ. Chem. Eng.*, 2021, **9**, 106380, DOI: [10.1016/J.JECE.2021.106380](https://doi.org/10.1016/J.JECE.2021.106380).

41 F. Farzin, M. K. Rofouei, M. Mousavi and J. B. Ghasemi, A novel Z-scheme oxygen-doped g-C<sub>3</sub>N<sub>4</sub> nanosheet/NaBiS<sub>2</sub> nanoribbon for efficient photocatalytic H<sub>2</sub>O<sub>2</sub> production and organic pollutants degradation, *J. Phys. Chem. Solids*, 2022, **163**, 110588, DOI: [10.1016/J.JPCS.2022.110588](https://doi.org/10.1016/J.JPCS.2022.110588).

42 A. Uddin, A. Rauf, T. Wu, R. Khan, Y. Yu, L. Tan, F. Jiang and H. Chen, In<sub>2</sub>O<sub>3</sub>/oxygen doped g-C<sub>3</sub>N<sub>4</sub> towards photocatalytic BPA degradation: balance of oxygen between metal oxides and doped g-C<sub>3</sub>N<sub>4</sub>, *J. Colloid Interface Sci.*, 2021, **602**, 261–273, DOI: [10.1016/J.JCIS.2021.06.003](https://doi.org/10.1016/J.JCIS.2021.06.003).

43 F. Mahdipour, M. Rafiee, B. Kakavandi, Z. Khazaee, F. Ghanbari, K. Y. Andrew Lin, S. Waclawek, A. Eslami and A. Bagheri, A new approach on visible light assisted oxygen doped g-C<sub>3</sub>N<sub>4</sub>/β-Bi<sub>2</sub>O<sub>3</sub> direct Z-scheme heterojunction towards the degradation of bisphenol A: degradation pathway, toxicity assessment, and continuous mode study, *Sep. Purif. Technol.*, 2022, **303**, 122171, DOI: [10.1016/J.SEPPUR.2022.122171](https://doi.org/10.1016/J.SEPPUR.2022.122171).

44 Z. Zhang, R. Ji, Q. Sun, J. He, D. Chen, N. Li, H. Li, A. Marcomini, Q. Xu and J. Lu, Enhanced photocatalytic degradation of 2-chlorophenol over Z-scheme heterojunction of CdS-decorated oxygen-doped g-C<sub>3</sub>N<sub>4</sub> under visible-light, *Appl. Catal., B*, 2023, **324**, 122276, DOI: [10.1016/J.APCATB.2022.122276](https://doi.org/10.1016/J.APCATB.2022.122276).

45 I. Tateishi, M. Furukawa, H. Katsumata and S. Kaneko, Photocatalytic degradation of bisphenol A using O-doped dual g-C<sub>3</sub>N<sub>4</sub> under visible light irradiation, *Catal. Today*, 2023, **411–412**, 113877, DOI: [10.1016/J.CATTOD.2022.08.019](https://doi.org/10.1016/J.CATTOD.2022.08.019).

46 W. Gan, J. Guo, X. Fu, J. Jin, M. Zhang, R. Chen, C. Ding, Y. Lu, J. Li and Z. Sun, Introducing oxygen-doped g-C<sub>3</sub>N<sub>4</sub> onto g-C<sub>3</sub>N<sub>4</sub>/TiO<sub>2</sub> heterojunction for efficient catalytic gatifloxacin degradation and H<sub>2</sub>O<sub>2</sub> production, *Sep. Purif. Technol.*, 2023, **317**, 123791, DOI: [10.1016/J.SEPPUR.2023.123791](https://doi.org/10.1016/J.SEPPUR.2023.123791).

